Author Manuscript

Author Manuscript

Author Manuscript

Author Manuscript

HHS Public Access

Author manuscript

*Melanoma Res*. Author manuscript; available in PMC 2021 February 01.

Published in final edited form as:

*Melanoma Res*. 2020 February ; 30(1): 52–61. doi:10.1097/CMR.0000000000000625.

# Enrichment of melanoma-associated T cells in 6-thioguanine-resistant T cells from metastatic melanoma patients

**Cindy L. Zuleger**[1], **Michael A. Newton**[1,2], **Xiuyu Ma**[2], **Irene M. Ong**[1,2,3], **Qinglin Pei**[4], **Mark R. Albertini**[1,5,6,7]

[1]University of Wisconsin Carbone Cancer Center;

[2]Department of Biostatistics and Medical Informatics, University of Wisconsin School of Medicine and Public Health, Madison, WI;

[3]Obstetrics and Gynecology, University of Wisconsin School of Medicine and Public Health, Madison, WI,

[4]Department of Biostatistics, University of Florida, Gainesville, FL;

[5]Department of Medicine University of Wisconsin School of Medicine and Public Health, Madison, WI;

[6]Medical Service, William S. Middleton Memorial Veterans Hospital, Madison, WI

## Abstract

**Objective:** Determine whether 6-thioguanine (TG) resistant T cells (mutant T cells (MT)) from metastatic melanoma patients (M-MEL) are enriched for melanoma-associated T cells compared to wild-type T cells (WT) obtained analogously without TG selection.

**Methods:** Melanoma-associated antigen (MAA) MHC Class I pentamer (P) staining was performed on MT and WT from 5 tumor and 9 peripheral blood samples from HLA-$A2^+$ M-MEL. T cell receptor (TCR) beta chain (TRB) repertoire was examined via Sanger sequencing of MT and WT in blood and tumor samples from M-MEL at times of tumor progression (n = 8) and via Illumina sequencing in melanoma tumor derived T cells and in T cells (uncultured (T0), WT and MT) obtained from blood before and after immune checkpoint blockade (Patient 20, n = 1).

**Results:** MT from tumor (3 of 5; $p<0.001$), but not blood (0 of 9), were enriched compared to WT for binding MAA-P. TRB analysis in M-MEL with tumor progression (n=8) detected increased melanoma-associated T cells in MT compared to WT from blood (Monte Carlo $p=10^{-7}$). Analysis of sequential blood samples from M-MEL before and after immune checkpoint blockade (Patient 20, n = 1) detected greater rates of TRB sharing between tumor and MT compared to tumor and WT or tumor and T0: 11.0% (72/656), 1.5% (206/13,639), and 1.3% (38½9,807), respectively (Monte Carlo $p=10^{-7}$ for MT vs WT and MT vs T0).

**Conclusions:** MT in M-MEL are enriched for melanoma-associated T cells and are candidate probes to study *in vivo* melanoma-reactive T cells.

[7]Please address reprint requests to corresponding author:Mark R. Albertini, MD, University of Wisconsin Clinical Sciences Center, Room K6/530, 600 Highland Avenue, Madison, WI 53792, Phone: 608-263-0117, Fax: 608-265-8133, mralbert@wisc.edu.

Author Manuscript Author Manuscript Author Manuscript Author Manuscript

**Keywords**

Melanoma; Cancer immunotherapy; Immune checkpoint blockade; Hypoxanthine-guanine phosphoribosyltransferase; Surrogate selection; T cell receptor beta

## Introduction

Exciting and impressive data with immune checkpoint blockade demonstrate the ability of the immune system to produce durable responses in some metastatic melanoma patients and have changed the standard of care [1,2]. Data emerging from human clinical trials suggest that checkpoint blockade is most effective for patients with tumors that already have T cell infiltration as well as for tumors that have a substantial somatic mutation burden in the tumor cells [3,4]. Metrics of broad TCR diversity and clonality have also been correlated with improved outcome following checkpoint blockade [5,6], as has upregulation of PD-L1 by the tumor [6]. In contrast, a recent analysis determined that effective immune checkpoint blockade results in a narrowing or focusing of the TCR repertoire [7]. However, additional measures of antitumor immune responses are needed to predict therapeutic efficacy and inform combination treatments as checkpoint blockade can be associated with substantial toxicity, is expensive, and has modest clinical antitumor response rates.

In melanoma, effective treatment with immune checkpoint blockade seems to require activation of anti-melanoma T cells specific for a wide variety of melanoma antigens including patient-unique neoantigens. Such activation is anticipated to stimulate *in vivo* clonal expansion of T cells, and consequently, the re-activation of functionally repressed T cells. As most mature T cells *in vivo* are in the quiescent $G_0$ stage of the cell cycle at any given time, selecting activated T cells, whether immunotherapy-induced or not, affords the opportunity to enrich, *ex vivo,* for a population of T cells participating in immunological processes, including anti-tumor effects and tumor regression. Spontaneous gene mutations arising *in vivo* in T cells are rare events, occurring primarily in activated and proliferating T cell subsets [8]. As such, *in vitro* selection for T cells with mutation in the hypoxanthine-guanine phosphoribosyltransferase (*HPRT*) gene enriches for rare *in vivo* activated proliferating T cells [8]. A loss-of-function mutation in *HPRT* results in resistance to TG, a cytotoxic purine analog. Thus, *in vivo HPRT* mutant (MT) T cells can be selected from peripheral blood or from sites of tumor by culturing lymphocytes *in vitro* in media containing TG. In contrast, wild-type (WT) T cells with a functional HPRT enzyme are killed in the presence of TG. *HPRT* MT T cells germane to T cell responses in immune mediated disorders have been found in patients with such diseases [8,9]. Melanoma is considered to be an immunogenic tumor, in part due to occurrences of spontaneous regressions as well as autoimmunity following successful immunotherapy or adoptive cell therapy [10–12]. Further, recent data suggest that brisk T cell infiltration into the tumor, so-called “hot” tumors, correlate with better response to immunotherapy [6]. We have used *HPRT* ‘surrogate selection’ to enrich for *in vivo* proliferating T cells in melanoma and hypothesize that *HPRT* MT T cells in metastatic melanoma patients are probes for T cells that can provide mechanistic insights into the *in vivo* immune response to melanoma [13–16].

Author Manuscript Author Manuscript Author Manuscript Author Manuscript

## Clinical Significance

There is a critical need to identify T cells in blood that have a role in the *in vivo* immune response to melanoma to inform the treatment of metastatic melanoma patients with immune checkpoint blockade. The candidate probe of *in vivo* TG-resistant T cells uses the biological effect of *in vivo* clonal proliferation to enrich for T cells responding to melanoma. Although the mutant fraction is presumably only a small fraction of any immunologically relevant T cell clone, this fraction serves to identify the larger clone by its specific TRB. This candidate probe merits additional investigation in metastatic melanoma and in other malignancies treated with immune checkpoint blockade.

## Materials and Methods

### Melanoma Patient biological specimens

This study was approved by the Health Sciences Institutional Review Board that serves the William S. Middleton Memorial Veterans Hospital (VA) and the University of Wisconsin (UW) Hospital and Clinics (UWHC). Written informed consent was obtained from all study participants. Eligibility requirements included a diagnosis of Stage III or Stage IV melanoma. HLA typing was performed by UWHC Histocompatibility Lab or by ProImmune for patients 1, 3, 5, 9, 13, 19, and 20. Expression of HLA-A2 was determined by flow cytometry with anti-HLA-A2 antibody (BB7.2, BD Bioscience (BD)) for patients 2, 4, 11, 16, 17, and 18. Twelve patients (Patients 1, 2, 3, 4, 5, 9, 11, 13, 16, 17, 18 and 19) provided samples between 2004 and 2007. An additional patient, hereto referred to as Patient 20, provided samples between 2008 and 2018. In 2008, an in-transit melanoma metastasis from Patient 20 was resected and processed for subsequent analysis. In 2010, Patient 20 was enrolled in a clinical trial involving intratumoral α-gal glycolipid (IT-AG) injections (IND 12946). The details of that trial were previously reported [17]. Briefly, the patient received two IT-AG injections given 4 weeks apart (0.1 mg/injection). Treatment outcome, determined 8 weeks after the first IT-AG injection, demonstrated disease progression. The patient then received Ipilimumab (3 mg/kg (capped at 125 kg)/dose every 3 weeks for 4 doses) beginning approximately 8 weeks after the second IT-AG injection. Blood samples were obtained pre-treatment on the day of the first IT-AG injection, 4 weeks after the second IT-AG injection, as well as 1-, 4-, and 13-months after the $4^{th}$ and final dose of Ipilimumab.

### Lymphocyte cloning assay and mass culture conditions

T cells were cloned as previously described [14,18]. Briefly, peripheral blood mononuclear cells (PBMC) were plated by limiting dilution into 96-well round-bottom plates in serum-free CTL Test Medium, with 10% lymphokine activated killer (LAK) cell supernatant (in-house generated exogenous IL-2 source), 20% HL-1, 5% FCS or HuAB and 0.25 μg/ml PHA (Remel, Lenexa, KS), with (MT) or without (WT) TG ($10^{-5}$ M) as the selection reagent. The 36×4 feeder cells, an *HPRT* deficient B cell line, were irradiated (90 Gy) and plated at $1 \times 10^4$ cells/well to stimulate T cell growth. Cloning efficiency (CE) and mutant frequency (MF) were calculated at Day 14 as described in the Statistical Analysis Section. Single-cell-derived T cell isolates were expanded in the above medium, with or without TG, and cryopreserved for subsequent molecular analyses. PBMC mass cultures were prepared

Author Manuscript Author Manuscript Author Manuscript Author Manuscript

using the same media components as cloning assay plates, but in bulk in T25 flasks, and were sub-cultured every 4 days, or as needed [14]. Melanoma tumor-infiltrating lymphocytes (TIL) or tumor-infiltrated lymph node (TILN) surgical specimens were mechanically and enzymatically disaggregated to single-cell suspensions as previously described, and mass cultures were prepared as for PBMC [14].

## Flow cytometry

### Melanoma Associated Antigen (MAA) MHC Class I pentamer (P) staining (Patients 2, 3, 4, 5, 11, 13, 16, 17, 19, 20)

Cells were incubated for 10 min at 25°C with 1 μg each of the following HLA-A*0201 pentamers pooled into one sample: $gp100_{209–217(210M)}$, $MelanA/MART\text{-}1_{26–35(27L)}$, $NY\text{-}ESO\text{-}1_{157–165(165V)}$, $Telomerase_{540–548}$, and $Tyrosinase_{369–377(371D)}$ (ProImmune, Oxford, UK). Cells were washed and counterstained with anti-CD3 (SK7, BD), and anti-CD8 (LT8, ProImmune) plus 2.5 tests of PE- or APC-labeled Fluorotag (ProImmune) for 20 min on ice. WT thresholds were used to establish the MT gating boundaries. Some samples were stained with HLA-A*0201 human T-cell lymphotropic virus-1 $Tax_{11–19}$ pentamer as a negative control. A TIL sample cultured with high-dose IL-2, soluble anti-CD3 (OKT3), and irradiated, allogeneic PBMC feeder cells, *i.e.*, rapid expansion protocol, was stained with the pooled MAA-P reagents as a positive control. DAPI (Sigma-Aldrich) or Live/Dead Fixable Violet (Invitrogen) were used to exclude dead cells, followed by examination of $CD3^+$ $CD8^+$ $pentamer^+$ cells. The gating strategy is shown in Supplementary Fig. 1, Supplemental Digital Content (SDC)-1. Data were acquired on a LSR II cytometer (BD) and analyzed with FlowJo software (version 10.5.3, FlowJo). Compensation was performed with BD Compensation Beads, Amine-Reactive Compensation Beads (Invitrogen), or cells.

### TRB sequencing

TRB from Patients 1, 2, 5, 9, 11, 13, 16, and 18 were sequenced using the Sanger method, and methods for RNA purification, PCR conditions, and primers were as previously published [14]. TRB from Patient 20 were sequenced on the Illumina platform as described herein. RNA was purified from uncultured (time zero, T0) PBMC or TIL, and from MT or WT mass cultures with Qiagen RNeasy Mini kits. Quantity and quality were assessed via QUBIT fluorometer and Agilent RNA Pico Chip on a 2100 BioAnalyzer, respectively. TRB cDNA libraries were prepared using Clontech SMARTer RACE 5’/3’ Kit with human TRB Constant gene specific primer 5’ caggcagtatctggagtcattgag. Following library preparation via Illumina TruSeq workflow, samples were sequenced using the Illumina MiSeq platform. TRB were collapsed to identical nucleotide sequences to enumerate T cell clones. IMGT nomenclature is used to describe TRB gene segments [19,20].

### Bioinformatics and Statistical Analysis

*HPRT* clonal assay data were processed by initially calculating a CE for each assay and a MF for each individual. To determine standard estimates for CE and MF, CE was calculated by use of the Poisson relationship, $P_0 = \exp(-x)$, where $P_0$ is the fraction of wells without colony growth and x is the average number of clonable cells per well. The value of x divided by the number of cells added to each well ($n_0$) defines the CE. The *HPRT* MF with this

Author Manuscript Author Manuscript Author Manuscript Author Manuscript

calculation is the ratio of the mean CE in the presence (selection (MT)) and absence (non-selection (WT)) of TG. Averaging yielded CE and MF values in cases with multiple dilutions.

To compare MT versus WT MAA-P frequencies, we used the conservative approach of Proschan *et al.* to account for the fact that the threshold gates are data dependent [21].

MiXCR was used to extract TCR clonotypes from Illumina MiSeq data [22] and consists of three primary steps: (1) an alignment where sequencing reads were aligned to reference V, D, J and C genes of TCR; (2) an assembly of clonotypes using alignments to identify specific gene regions (e.g. complementarity determining region 3 (CDR3)); and (3) export of the clonotypes for inspection. Our MiXCR (v2.1.1) analysis followed the workflow recommended by Bolotin et al [22] except that we invoked the option '-OallowPartialAlignments=true' to prevent MiXCR from filtering out partial alignments that did not fully cover CDR3. This modification was needed as our data was based on randomly sheared cDNA libraries created for RNASeq. To reconstruct full CDR3 sequences where possible, two rounds of contig assembly were performed using the available alignments. Clonotypes were then assembled, exported to a text file, and alignment fidelity was assessed manually.

Variation characteristics of empirical TRB frequencies invalidate the use of simple statistical procedures, such as Fisher's exact test, to compare proportions. MT sequence counts are subject to sources of extra-multinomial variation caused by population bottleneck and growth variation *in vitro* [23]. We limit the impact of this problem by considering only distinct sequences and their occurrence or co-occurrence in multiple samples, and ignoring full frequency information that would reveal sequencing depth. A second problem is that we compare TRB rates among populations where a given sequence is on both sides of the equation: i.e., a given sequence may occur both in WT and tumor and in MT and tumor, and so empirical frequencies (over TRB's) are not independent binomial proportions. A third problem is that the indicators of occurrence of a given TRB in the various samples are positively correlated owing to shared biological features. Specifically, a large TRB clone having relatively high detection rate in the WT class is predicted to also be relatively easy to detect in the MT and tumor classes, just because of its size, in the absence of any fundamental differences among the WT, MT, or tumor classes. Addressing these issues, we developed a statistical approach to measure the enrichment of tumor-associated TRB's in MT as compared to WT cells, details of which are provided in the accompanying Statistical Supplement (see text document, SDC-2). This approach was used to analyze both Sanger and Illumina datasets.

UpSetR was used to plot data intersections [24].

## Results

### Patient characteristics and biological samples

Patient and biological samples are described in Table 1. The PBMC and tumor samples were obtained near the time of clinically indicated surgery for progressive metastatic melanoma

Author Manuscript Author Manuscript Author Manuscript Author Manuscript

for Patients 1, 2, 3, 4, 5, 9, 11, 13, 16, 17, 18, and 19. A baseline tumor sample and serial blood samples beginning 20 months later were collected from Patient 20 (Supplementary Fig. 2, SDC-3).

### Patient 20 *HPRT* cloning assays and mass cultures

CE and MF were calculated from four of the five PBMC cloning assays from Patient 20 (Supplementary Table 1, SDC-4). The CE (%) for Baseline, Post-IT-AG, 1-month Post-Ipi, and 13-months Post-Ipi were 12.4, 6.4, 26.6, and 10.6, respectively; the MF (x $10^{-6}$) for the same timepoints were 114.3, 88.4, 23.1, and 87.1, respectively. The 4-month Post-Ipi assay failed to yield viable T cell clones for either WT or MT, thus the 4-month Post-Ipi CE and MF could not be determined. Calculated MF values varied among the different sample timepoints, but all were elevated compared to the mean background value for a large cohort of adult males [25]. Mass cultures were prepared successfully for all five PBMC samples. The details of the mass cultures and the RNA quality control are presented in Supplementary Table 2, SDC-5. TRB data from Patient 20 are from mass cultures.

### Flow Cytometry

Mass cultures from five tumor and nine blood samples from HLA-A2$^+$ melanoma patients were stained with HLA-A2 MAA peptide pentamers (Table 2). As these experiments were intended as a screening tool and the biological materials were limited, the five pentamer reagents were pooled. Representative results obtained using Patient 16's MT and WT TILN are shown in Fig. 1. The MT TILN contain an antigen-specific population of 1.51% of live CD8$^+$ lymphocytes detected by the pool of five MAA pentamers, a 45-fold enrichment compared to WT TILN ($p < 0.001$). A significant enrichment of melanoma-specific T cells in MT compared to WT was also found in a TIL mass culture from Patients 11 and in one of two TILN mass cultures from Patient 13 (3 of 5 total) ($p < 0.001$), despite both of these samples having very low numbers of total CD3$^+$ CD8$^+$ T cells (Table 2). The finding of increased pentamer$^+$ events in the MT compared to the WT did not extend to the blood mass cultures examined (0 out of 9) (Table 2). Neither the MT nor WT peripheral blood mass cultures from Patient 20 demonstrated substantial MAA pentamer$^+$ T cells (Table 2). Pentamer staining of Patient 20's TIL was not performed due to limited sample.

### Sharing of TRB sequences with tumor-derived lymphocytes is greater in MT compared to WT

Sanger sequencing revealed a total of 1,712 distinct TRB in the tumor, MT and WT from eight patients with metastatic melanoma (Patients 1, 2, 5, 9, 11, 13, 16, and 18). There were 544, 359, and 792 TRB found only in the tumor, MT or WT, respectively. While no TRB were found across all three subsets (tumor, MT and WT), there were 7, 2, and 2 TRB found in common between tumor and MT, tumor and WT, or MT and WT, respectively (Table 3). Due to the low read counts per patient, sequences were pooled over the eight patients and significantly greater MT sequences were shared with tumor-derived lymphocytes than were WT sequences (Monte Carlo $p=10^{-7}$, MT vs WT, Table 3).

Author Manuscript Author Manuscript Author Manuscript Author Manuscript

### Clonotypic diversity is reduced in MT compared to WT or T0

RNA from serial blood samples from T0, WT, and MT from Patient 20 was sequenced via Illumina MiSeq to examine changes in TRB repertoire diversity longitudinally as well as across culture conditions. RNA from TIL collected 20-months prior to IT-AG (T-T0) was also sequenced. A distinct clone is defined by sequence identity across the TRB Variable (TRBV) gene, CDR3 nucleotide sequence, and TRB Joining (TRBJ) gene. Relatively similar numbers of total TRB sequences were obtained across all 16 multiplexed samples (Supplementary Table 2, SDC-5). The total TRB include multiple occurrences of distinct clones, *i.e.,* the total number enumerates the count of all occurrences of distinct TRB sequences found as singlets and those found multiple times. However, we identified a highly skewed distribution of distinct TRB sequences when comparing T0 or WT with MT from the same sample (Supplementary Table 2, SDC-5). The low numbers of distinct TRB sequences in MT (identifying *in vivo* clones) were similar across the five samples (Supplementary Table 2, SDC-5). Variation in number of distinct sequences was not attributed to RNA quality or quantity.

### Sharing of TRB sequences with TIL is greater in MT compared to WT or T0

TRB with identical nucleotide sequences and TRBV genes were found shared across several of Patient 20's timepoints. The detection rate of TRB shared between T-T0 and MT, considering all timepoints, was 11.0% (72/656). This rate of TRB sharing between T-T0 and MT was higher than the rate of TRB sharing between T-T0 and either WT or T0, 1.5 % (206/13,639), and 1.3 % (38½9,807), respectively ($p=10^{-7}$, Monte Carlo computations for MT vs WT and MT vs T0 comparisons) (Table 4). This trend of increased TRB sharing between MT and T-T0 was also detected when applied to persisting clones (*i.e.,* clones present at more than one peripheral blood timepoint). The detection rate of TRB shared between the T-T0 and persisting MT, was 43.6% (17/39). This rate of TRB sharing between T-T0 and MT was higher than between the rate of TRB sharing between T-T0 and either WT or T0, 16.0 % (87/544), and 8.6 % (192/2,231), respectively ($p=10^{-4}$, Monte Carlo computations for MT vs WT and MT vs T0 comparisons) (Table 4). TRB sharing was detected across the time course of this study with identical T0 and WT clones identified at 2, 3, 4, and 5 different timepoints (Fig. 2a–b). Despite the overall lower numbers of distinct TRB defined clones, a similar profile was noted for MT clones, with identical clones identified at 2, 3, and 4 different timepoints (Fig. 2c).

## Discussion

The identification of probes for *in vivo* melanoma-reactive T cells in metastatic melanoma patients could have a significant impact on patient management. We have previously shown that *HPRT* surrogate selection can identify *in vivo* expanding T cell clones in melanoma patients that can traffic to tumor within an individual melanoma patient and have public TRB between different melanoma patients [14,15]. Some *HPRT* MT T cells have similar TRB sequences as melanoma-specific T cells identified in a literature-derived empirical database [15]. We hypothesized that *HPRT* surrogate selection would enrich for the biological event of *in vivo* T cell clonal amplification and identify T cells mediating antitumor responses following immune checkpoint blockade for metastatic melanoma. We

Author Manuscript Author Manuscript Author Manuscript Author Manuscript

now report that MT T cells in the blood of metastatic melanoma patients have increased melanoma-associated T cells compared to WT. In addition, MAA-specific T cells from sites of tumor can be detected in MT T cells using flow cytometry.

Pentamer staining of MT T cells identified enrichment of MAA-specific T cells from tumor sites (3 of 5 samples from 4 patients), but not in PBMC of nine patients (0 of 9 samples). It is noted that these analyses were limited to five HLA-A2-binding peptides and a relatively small number of patients. The T cell response to melanoma is broad, encompassing multiple HLA alleles and both public epitopes and private neoantigens, and including CD4 as well as CD8 T cells. Thus, the HLA-A*0201-binding peptide reagents used herein represent only a fraction of the epitopes targeted by T cells. Despite this limitation, our data agree with other reports of a higher frequency of MAA-reactive T cells in the tumor microenvironment compared to the circulation [26].

We initially examined MT and WT TRB from the blood and from the tumor of eight metastatic melanoma patients with tumor progression and detected increased melanoma-associated T cells (*i.e.*, TRB matches between blood and tumor) in MT compared to WT using Sanger methodology. Sanger data are much lower throughput, and consequently depth, than those of the Illumina platform. Thus, we used the Illumina platform to study serial MT and WT samples and identified enrichment of melanoma-associated T cells in MT in a metastatic melanoma patient (Patient 20) who achieved durable antitumor benefit following treatment with immune checkpoint blockade. It is important to note that Patient 20's data were obtained from initial samples during tumor progression and from subsequent samples during tumor regression. Several T cell clones were present over the course of this patient's disease. Since MT from the blood of metastatic melanoma patients are enriched for melanoma-associated T cells, they are candidate probes for mechanistic studies to identify antimelanoma T cells in blood. Additional study of phenotypic, functional, and quantitative differences of MT between patients with disease regression and disease progression is needed in a larger cohort of metastatic melanoma patients to assess whether MT from the blood of metastatic melanoma patients could function as a biomarker of antitumor response.

While the *HPRT* MF measurements in the serial blood samples from Patient 20 are greater than values typically seen in normal controls [13,25], our study was not designed to compare CE or MF to normal controls, either directly or retrospectively. Moreover, previous reports of lower CE of patient blood samples compared to normal controls [13], whether due to biologic or technical factors, cautions over-interpretation of these values. Assay variability and small sample size do not allow conclusions about the change in *HPRT* MF following immune checkpoint blockade. In addition, it is important to emphasize that MFs (mutant frequency, measured in this study) are not mutation frequencies. MFs reflect accumulation of mutants at any given time, whereas mutation frequencies reflect mutation events occurring at any given time [25]. The magnitude of MFs is likely only a rough indicator of immunological activity.

TRB sequences from an in-transit melanoma metastasis obtained ~20 months before Patient 20 received IT-AG (T-T0) were followed in serial blood samples to determine if these tumor-associated TRB sequences persisted in the blood of a responding melanoma patient.

Author Manuscript Author Manuscript Author Manuscript Author Manuscript

Although it is not known whether these MT participated in the antitumor response, analysis of the fresh tumor (T-T0) revealed that TRB clones found in the tumor were detected in MT in the circulation throughout the disease course and years following a complete response. Moreover, a statistically higher percentage of TRB present in T-T0 were also found as MT clones compared to T0 or WT. Overlapping T cell clones in the blood and tumor of melanoma patients responding to novel immunotherapies have been reported [27,28]. Similar observations of shared TRB in the blood and tumor of patients with various cancers responding to immune checkpoint blockade have been reported [26,29,30]. It is important to note that selection with TG selects for only a subset of the TRB clones that were found in the tumor. Conversely, the WT culture, although expanding many bystander TRB clones, would be expected to contain some tumor-related TRB that were only found in WT expanded TRB and lost in cultures expanded with TG selection. Additional study is needed to determine whether tumor-related TRB that are present in T cells cultured in WT conditions and lost in MT conditions are relevant for tumor immunity. We hypothesize that TRB relevant to the *in vivo* antimelanoma T cell response will be enriched in MT cultures compared to WT cultures. We further hypothesize that *HPRT* mutant T cells are not *per se* the mediators of the relevant immune responses but serve to identify the clones mediating the *in vivo* antitumor response. The mutant fraction of any clone is presumably only a tiny fraction of that *in vivo* clone.

Several strategies can be used for TCR repertoire analysis [31–34]. Our workflow converted total RNA into cDNA with a focus on TRB as a marker of T cell clonality. It is important to emphasize that this analysis quantified TRB sequences – not cells – because we measured sequences identified from RNA. While this may provide a rough indicator of numbers of cells, there could be great distortions due to differing RNA production among the cells. The tumor sample was from freshly disaggregated tissue and no excess sample was available for exome sequencing and neoantigen prediction to determine the mutational landscape of the tumor. We were also unable to access either formalin-fixed paraffin-embedded tissue blocks or slides from which to macro-dissect cells for isolation of RNA or DNA. However, study findings demonstrate that *HPRT* surrogate selection can identify subdominant ‘rare’ T cells in a melanoma patient at the time of tumor regression. We also found TRB from TIL obtained over 2 years before Ipilimumab in MT in the blood following an antitumor response to Ipilimumab, and those TRB were enriched in MT compared to WT and T0. An important highlight of the *HPRT* methodology is the ability to detect T cell clones which may be missed by traditional sequencing of T0 samples, due to the extensive sequencing depth necessary for such rare T cell detection. Despite the higher numbers of unique clones in T0 or WT compared to MT, clones were revealed in MT that were undetectable in either T0 or WT. Moreover, because *HPRT* surrogate selection does not rely on a preconceived ‘relevant’ antigen, it follows that T cells specific to novel tumor-associated antigens could be identified. We are proceeding with functional experiments to study the role of these emerging MT in the response to melanoma and will examine whether MT provide a probe for tumor-rejection epitopes that could identify novel therapeutic targets.

Limitations of our study include the analysis of pooled T cell populations and the modest depth of sequencing. Further, expansion rates of T cell subsets are not all equivalent and *in vitro* growth may alter the repertoire [35]. Exhaustive deep sequencing of purified T cell

Author Manuscript Author Manuscript Author Manuscript Author Manuscript

subsets, droplet-based microfluidic separation, and combined proteomic and transcriptomic profiling techniques [32,36,37] may be required to reveal and elucidate the phenotypic and functional properties of the selected *HPRT* MT T cells. While we cannot yet make conclusions as to the functional profile of any specific CDR3 sequence, such experiments are planned. In summary, *HPRT* surrogate selection may afford the opportunity to identify rare melanoma-associated T cells, as well as antigens triggering *in vivo* T cell activation, that remain undetected through current bioinformatic pipelines [38,39].

## Conclusion

*HPRT* surrogate selection merits additional study in metastatic melanoma patients treated with immune checkpoint blockade to identify *in vivo* melanoma-reactive T cells.

## Supplementary Material

Refer to Web version on PubMed Central for supplementary material.

## Acknowledgements

The authors thank the UW Carbone Cancer Center for use of its facilities and services and the nurses on the UW Clinical Research Unit for outstanding nursing care and clinical trial support. We thank Michael D. Macklin for technical assistance and Laddie Johnson for assistance with manuscript preparation. The authors also thank Dr. Richard J. Albertini (University of Vermont) for thoughtful discussions and for review of this manuscript.

Conflicts of Interest and Source of Funding: The authors have no financial or other conflicts of interest to disclose related to this publication. This work was supported by the National Cancer Institute under Grant P30 CA014520; and by resources at the William S. Middleton Memorial Veterans Hospital, Madison, WI. The content is solely the responsibility of the authors and does not necessarily represent the official views of the NIH or the views of the Dept. of Veterans Affairs or the United States Government. Additional support was provided by Ann's Hope Foundation, Taking On Melanoma, the Tim Eagle Memorial, the Jay Van Sloan Memorial from the Steve Leuthold Family, and the Gretchen and Andrew Dawes Charitable Trust.

## References

1. Sharma P, Allison JP. The future of immune checkpoint therapy. Science 2015; 348: 56–61. [PubMed: 25838373]
2. Albertini MR. The age of enlightenment in melanoma immunotherapy. J Immunother Cancer 2018; 6: 80. [PubMed: 30134977]
3. Rizvi NA, Hellmann MD, Snyder A, Kvistborg P, Makarov V, Havel JJ, et al. Cancer immunology. Mutational landscape determines sensitivity to PD-1 blockade in non-small cell lung cancer. Science 2015; 348: 124–128. [PubMed: 25765070]
4. Ledford H Sizing up a slow assault on cancer. Nature 2013; 496: 14. [PubMed: 23552923]
5. Cha E, Klinger M, Hou Y, Cummings C, Ribas A, Faham M, et al. Improved survival with T cell clonotype stability after anti-CTLA-4 treatment in cancer patients. Sci Transl Med 2014; 6: 238ra270.
6. Tumeh PC, Harview CL, Yearley JH, Shintaku IP, Taylor EJ, Robert L, et al. PD-1 blockade induces responses by inhibiting adaptive immune resistance. Nature 2014; 515: 568–571. [PubMed: 25428505]
7. Sidhom JW, Bessell CA, Havel JJ, Kosmides A, Chan TA, Schneck JP. ImmunoMap: A Bioinformatics Tool for T-cell Repertoire Analysis. Cancer Immunol Res 2018; 6: 151–162. [PubMed: 29263161]
8. Albertini RJ. HPRT mutations in humans: biomarkers for mechanistic studies. Mutat Res 2001; 489: 1–16. [PubMed: 11673087]

Author Manuscript Author Manuscript Author Manuscript Author Manuscript


9. Allegretta M, Nicklas JA, Sriram S, Albertini RJ. T cells responsive to myelin basic protein in patients with multiple sclerosis. Science 1990; 247: 718–721. [PubMed: 1689076]
10. Yeh S, Karne NK, Kerkar SP, Heller CK, Palmer DC, Johnson LA, et al. Ocular and systemic autoimmunity after successful tumor-infiltrating lymphocyte immunotherapy for recurrent, metastatic melanoma. Ophthalmology 2009; 116: 981–989 e981. [PubMed: 19410956]
11. Oyarbide-Valencia K, van den Boorn JG, Denman CJ, Li M, Carlson JM, Hernandez C, et al. Therapeutic implications of autoimmune vitiligo T cells. Autoimmun Rev 2006; 5: 486–492. [PubMed: 16920575]
12. Mukherji B, Nathanson L, Clark DA. Studies of humoral and cell-mediated immunity in human melanoma. Yale J Biol Med 1973; 46: 681–692. [PubMed: 4130586]
13. Albertini MR, King DM, Newton MA, Vacek PM. In vivo mutant frequency of thioguanine-resistant T-cells in the peripheral blood and lymph nodes of melanoma patients. Mutat Res 2001; 476: 83–97. [PubMed: 11336986]
14. Albertini MR, Macklin MD, Zuleger CL, Newton MA, Judice SA, Albertini RJ. Clonal expansions of 6-thioguanine resistant T lymphocytes in the blood and tumor of melanoma patients. Environ Mol Mutagen 2008; 49: 676–687. [PubMed: 18712786]
15. Zuleger CL, Macklin MD, Bostwick BL, Pei Q, Newton MA, Albertini MR. In vivo 6-thioguanine-resistant T cells from melanoma patients have public TCR and share TCR beta amino acid sequences with melanoma-reactive T cells. J Immunol Methods 2011; 365: 76–86. [PubMed: 21182840]
16. Zuleger CL, Albertini MR. OMIP-008: measurement of Th1 and Th2 cytokine polyfunctionality of human T cells. Cytometry A 2012; 81: 450–452. [PubMed: 22431369]
17. Albertini MR, Ranheim EA, Zuleger CL, Sondel PM, Hank JA, Bridges A, et al. Phase I study to evaluate toxicity and feasibility of intratumoral injection of alpha-gal glycolipids in patients with advanced melanoma. Cancer Immunol Immunother 2016; 65: 897–907. [PubMed: 27207605]
18. O'Neill JP, McGinniss MJ, Berman JK, Sullivan LM, Nicklas JA, Albertini RJ. Refinement of a T-lymphocyte cloning assay to quantify the in vivo thioguanine-resistant mutant frequency in humans. Mutagenesis 1987; 2: 87–94. [PubMed: 3331707]
19. Lefranc MP, Giudicelli V, Kaas Q, Duprat E, Jabado-Michaloud J, Scaviner D, et al. IMGT, the international ImMunoGeneTics information system. Nucleic Acids Res 2005; 33: D593–597. [PubMed: 15608269]
20. Lefranc M-P, Lefranc G. The T Cell Receptor Factsbook, London, UK: Academic Press, 2001.
21. Proschan MA, Nason M. Conditioning in 2 × 2 tables. Biometrics 2009; 65: 316–322. [PubMed: 18505423]
22. Bolotin DA, Poslavsky S, Mitrophanov I, Shugay M, Mamedov IZ, Putintseva EV, et al. MiXCR: software for comprehensive adaptive immunity profiling. Nat Methods 2015; 12: 380–381. [PubMed: 25924071]
23. Pei Q, Zuleger CL, Macklin MD, Albertini MR, Newton MA. A conditional predictive p-value to compare a multinomial with an overdispersed multinomial in the analysis of T-cell populations. Biostatistics 2014; 15: 129–139. [PubMed: 24096387]
24. Conway JR, Lex A, Gehlenborg N. UpSetR: an R package for the visualization of intersecting sets and their properties. Bioinformatics 2017; 33: 2938–2940. [PubMed: 28645171]
25. Albertini RJ, Vacek PM, Carter EW, Nicklas JA, Squibb KS, Gucer PW, et al. Mutagenicity monitoring following battlefield exposures: Longitudinal study of HPRT mutations in Gulf War I veterans exposed to depleted uranium. Environ Mol Mutagen 2015; 56: 581–593. [PubMed: 25914368]
26. Gros A, Parkhurst MR, Tran E, Pasetto A, Robbins PF, Ilyas S, et al. Prospective identification of neoantigen-specific lymphocytes in the peripheral blood of melanoma patients. Nat Med 2016; 22: 433–438. [PubMed: 26901407]
27. Aris M, Bravo AI, Pampena MB, Blanco PA, Carri I, Koile D, et al. Changes in the TCRbeta Repertoire and Tumor Immune Signature From a Cutaneous Melanoma Patient Immunized With the CSF-470 Vaccine: A Case Report. Front Immunol 2018; 9: 955. [PubMed: 29774030]
28. Bajor DL, Xu X, Torigian DA, Mick R, Garcia LR, Richman LP, et al. Immune activation and a 9-year ongoing complete remission following CD40 antibody therapy and metastasectomy in a

Author Manuscript Author Manuscript Author Manuscript Author Manuscript

patient with metastatic melanoma. Cancer Immunol Res 2014; 2: 1051–1058. [PubMed: 25252722]

29. Forde PM, Chaft JE, Smith KN, Anagnostou V, Cottrell TR, Hellmann MD, et al. Neoadjuvant PD-1 Blockade in Resectable Lung Cancer. N Engl J Med 2018; 378: 1976–1986. [PubMed: 29658848]
30. Huang AC, Postow MA, Orlowski RJ, Mick R, Bengsch B, Manne S, et al. T-cell invigoration to tumour burden ratio associated with anti-PD-1 response. Nature 2017; 545: 60–65. [PubMed: 28397821]
31. Klein AM, Mazutis L, Akartuna I, Tallapragada N, Veres A, Li V, et al. Droplet barcoding for single-cell transcriptomics applied to embryonic stem cells. Cell 2015; 161: 1187–1201. [PubMed: 26000487]
32. Macosko EZ, Basu A, Satija R, Nemesh J, Shekhar K, Goldman M, et al. Highly Parallel Genome-wide Expression Profiling of Individual Cells Using Nanoliter Droplets. Cell 2015; 161: 1202–1214. [PubMed: 26000488]
33. Robins HS, Campregher PV, Srivastava SK, Wacher A, Turtle CJ, Kahsai O, et al. Comprehensive assessment of T-cell receptor beta-chain diversity in alphabeta T cells. Blood 2009; 114: 4099–4107. [PubMed: 19706884]
34. Shugay M, Britanova OV, Merzlyak EM, Turchaninova MA, Mamedov IZ, Tuganbaev TR, et al. Towards error-free profiling of immune repertoires. Nat Methods 2014; 11: 653–655. [PubMed: 24793455]
35. Gattinoni L, Klebanoff CA, Restifo NP. Paths to stemness: building the ultimate antitumour T cell. Nat Rev Cancer 2012; 12: 671–684. [PubMed: 22996603]
36. Stoeckius M, Hafemeister C, Stephenson W, Houck-Loomis B, Chattopadhyay PK, Swerdlow H, et al. Simultaneous epitope and transcriptome measurement in single cells. Nat Methods 2017; 14: 865–868. [PubMed: 28759029]
37. Shahi P, Kim SC, Haliburton JR, Gartner ZJ, Abate AR. Abseq: Ultrahigh-throughput single cell protein profiling with droplet microfluidic barcoding. Sci Rep 2017; 7: 44447. [PubMed: 28290550]
38. Dash P, Fiore-Gartland AJ, Hertz T, Wang GC, Sharma S, Souquette A, et al. Quantifiable predictive features define epitope-specific T cell receptor repertoires. Nature 2017; 547: 89–93. [PubMed: 28636592]
39. Shugay M, Bagaev DV, Zvyagin IV, Vroomans RM, Crawford JC, Dolton G, et al. VDJdb: a curated database of T-cell receptor sequences with known antigen specificity. Nucleic Acids Res 2018; 46: D419–d427. [PubMed: 28977646]

Author Manuscript Author Manuscript Author Manuscript Author Manuscript

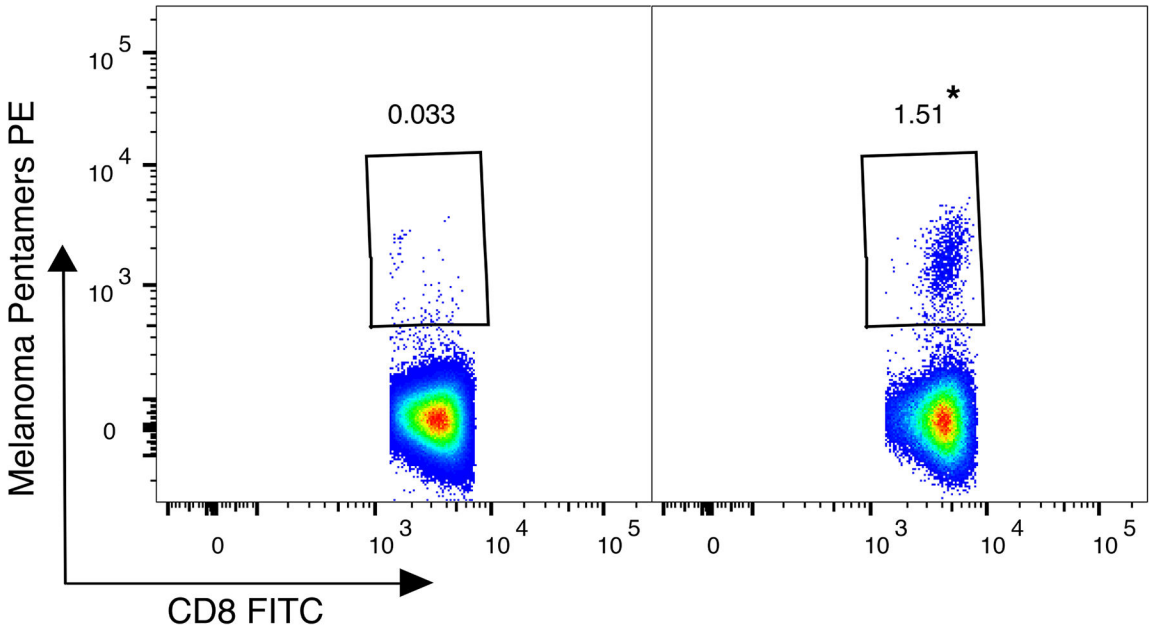


**Fig. 1.**

Patient 16 MT cultured from tumor-infiltrated lymph node (TILN) contains a melanoma associated antigen (MAA)-specific population. WT (left) and MT (right) TILN were incubated with HLA-A*0201 pentamers and co-stained for CD3 and CD8. Numbers in plots represent the frequency of MAA pentamer$^+$ cells of total CD3$^+$ CD8$^+$ T cells. * frequency of MAA pentamer$^+$ in MT was significantly greater than in WT ($p < 0.001$), modified Proschan's method (Materials and Methods).

Author Manuscript
Author Manuscript
Author Manuscript
Author Manuscript



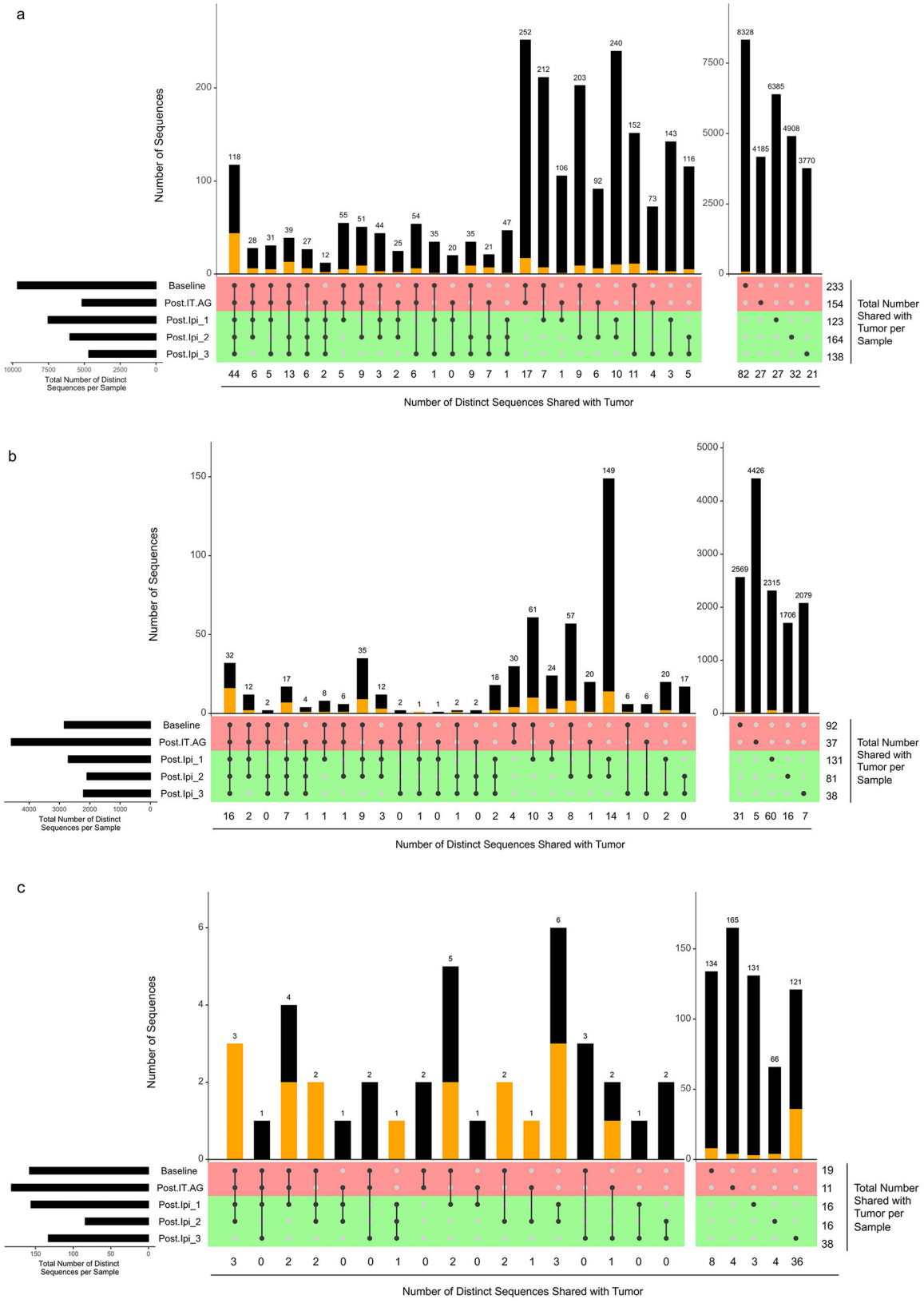


**Fig. 2.**

Author Manuscript Author Manuscript Author Manuscript Author Manuscript

UpSetR plot of distinct TRB CDR3 sequences across five peripheral blood samples from Patient 20 at T0 **(a)**, WT **(b)**, and MT **(c)**. Identification of identical CDR3 sequences at different timepoints is shown as a matrix in which the rows represent the mass cultures at each timepoint and the columns represent their intersection. For each sequence that is part of a given intersection, a black filled circle is placed in the corresponding matrix cell. Empty intersections are shown as a light gray circle. The vertical black lines connect the topmost black circle to the bottommost black circle in each column. The number of identical CDR3 identified at the different timepoints is shown as the bar chart at the top of the matrix, and the number of such sequences also shared with the tumor is presented below the plot, as well as represented by the orange segment in the bar chart. The remaining (*i.e.*, not shared with the tumor) sequences are represented by the black segment in the bar chart. The total number of CDR3 shared with the tumor per timepoint is presented to the right of the plot. The top two rows (colored red) and the bottom three rows (colored green) of the matrix correspond to times of tumor growth and regression, respectively. The horizontal bar plot, to the left of the matrix, shows the number of distinct sequences per sample. Post-IT.AG, Post-intratumoral alpha-gal glycolipids; Ipi, Ipilimumab; Post.Ipi_1, _2, _3 correspond to 1 month, 4 months, and 13 months Post-Ipi, respectively.

Author Manuscript Author Manuscript Author Manuscript Author Manuscript

**Table 1.**

Melanoma patient characteristics and assay details.

| Patient ID | Age[a] | Sex | Stage of Disease[b] | Biological Samples[c] | |
|---|---|---|---|---|---|
| 1 | 70.2 | M | III | PBMC[d] | TILN[d] |
| 2 | 44.6 | M | IV | PBMC[d,e] | TIL[d] |
| 3 | 36.4 | M | IV | PBMC[e] | n/d |
| 4 | 36.3 | M | IV | PBMC[e] | n/d |
| 5 | 55.5 | M | IV | PBMC[d,e] | TIL[d] |
| 9 | 71.3 | M | IV | PBMC[d] | TIL-1[d] TIL-2[d] |
| 11[f] | 58.1 | F | IV | PBMC-1[d] PBMC-2[d,e] | TIL[d,e] |
| 13[g] | 69.6 | M | IV | PBMC[d,e] | TILN-1[d,e] TILN-2[d,e] |
| 16 | 45.8 | M | III | PBMC[d,e] | TIL[d,e] |
| 17 | 81.3 | M | IV | n/d | TIL[e] |
| 18 | 54.8 | F | IV | PBMC[d] | TILN[d] |
| 19 | 60.3 | M | IV | PBMC[e] | n/d |
| 20 | 57.0 | M | III | PBMC[e]<br>PBMC (Baseline)[h]<br>PBMC (Post-IT-AG)[h]<br>PBMC (Post-Ipi-1)[h]<br>PBMC (Post-Ipi-2)[h]<br>PBMC (Post-Ipi-3)[h] | TIL (T-T-0)[h,i] |

[a] Age at time of initial blood sample acquisition for all patients except Patient 17, which refers to the age at time of tumor resection.

[b] AJCC stage refers to the stage of disease at the time of initial blood sample acquisition for all except Patient 17, which refers to the stage of disease at the time of tumor resection.

[c] PBMC were obtained near the time of clinically indicated surgery to obtain TIL or TILN for Patients 1, 2, 3, 4, 5, 9, 11, 13, 16, 17, 18, and 19, or at several timepoints beginning 20 months after resection of an in-transit metastasis (Patient 20).

[d] TRB Sanger sequencing.

[e] MAA peptide pentamer flow cytometry; Patients were HLA-A2$^{+}$, except Patients 1 and 9.

[f] Two blood samples collected ~2 year apart.

[g] Two anatomically distinct TIL obtained on the same date.

[h] TRB Illumina sequencing.

[I] IFN-γ ICS.

AJCC, American Joint Committee on Cancer; PBMC, Peripheral blood mononuclear cells; TIL, tumor-infiltrating lymphocytes; TILN, tumor-infiltrated lymph node n/d, sample not analyzed

Author Manuscript Author Manuscript Author Manuscript Author Manuscript

**Table 2.**

Melanoma patient and sample characteristics, and HLA-A*0201 melanoma-associated antigen pentamer data.

| Patient ID[a] | Age[b] | Sample source | MT | | | WT | | |
|---|---|---|---|---|---|---|---|---|
| | | | # $CD3^+$ $CD8^+$ $Pentamer^+$ T cells | # Total $CD3^+$ $CD8^+$ T cells | % $CD3^+$ $CD8^+$ $Pentamer^+$ | # $CD3^+$ $CD8^+$ $Pentamer^+$ T cells | # Total $CD3^+$ $CD8^+$ T cells | % $CD3^+$ $CD8^+$ $Pentamer^+$ |
| 2 | 44.6 | PBMC | 0 | 22,579 | 0 | 1 | 31,860 | 0.003 |
| 3 | 36.4 | PBMC | 0 | 52,035 | 0 | 120 | 99,126 | 0.12 |
| 4 | 36.3 | PBMC | 52 | 49,817 | 0.10 | 84 | 47,397 | 0.18 |
| 5 | 55.5 | PBMC | 6 | 10,759 | 0.06 | 33 | 50,362 | 0.07 |
| 11 | 58.1 | PBMC | 9 | 61,178 | 0.01 | 23 | 143,131 | 0.02 |
| | | TIL | 3 | 107 | 2.8* | 22 | 68,611 | 0.03 |
| 13 | 69.6 | PBMC | 5 | 77,809 | 0.01 | 6 | 53,777 | 0.01 |
| | | TILN-1[c] | 6 | 1,452 | 0.41* | 4 | 100,677 | 0.004 |
| | | TILN-2[c] | 16 | 128,326 | 0.01 | 7 | 160,979 | 0.004 |
| 16 | 45.8 | PBMC | 25 | 236,129 | 0.01 | 19 | 256,400 | 0.01 |
| | | TILN | 991 | 65,601 | 1.51* | 87 | 267,569 | 0.03 |
| 17 | 81.3 | TIL | 12 | 229,553 | 0.01 | 8 | 140,029 | 0.01 |
| 19 | 60.5 | PBMC | 18 | 283,938 | 0.01 | 95 | 132,098 | 0.07 |
| 20 | 57.0 | PBMC | 14 | 44,282 | 0.03 | 0 | 18,673 | 0 |

[a] Patient ID assigned internally and reflects chronological order of analyzed samples. All patients were male except patient 11. All patients had Stage IV metastatic melanoma except patients 16 and 20, who had Stage III metastatic melanoma.

[b] Age at time of initial blood sample acquisition for all patients except Patient 17, which is the age at time of tumor resection.

[c] Two anatomically distinct TILN obtained on the same date were analyzed.

PBMC, peripheral blood mononuclear cells; TILN, tumor-infiltrated lymph node; TIL, tumor infiltrating lymphocytes

* $p<0.001$, $pentamer^+$ frequency MT compared to WT

Author Manuscript

Author Manuscript

Author Manuscript

Author Manuscript

**Table 3.**

Sharing of MT and WT TRB sequences with tumor in Sanger sequence data set.

| $n_{111}$ | $n_{110}$* | $n_{101}$* | $n_{100}$ | $n_{011}$ | $n_{010}$ | $n_{001}$ |
|---|---|---|---|---|---|---|
| 0 | 7 | 2 | 544 | 2 | 359 | 792 |

Sanger sequence data from 8 patients were collapsed into 3 sets: tumor, MT, or WT. Clonotypes had identical TRBV, CDR3, and TRBJ. The number of sequences shared between sets is represented by ‘n’, and the subscripts represent tumor, MT, and WT, respectively.

MT mutant; WT; wild-type; TRB, T cell receptor beta; TRBV, TRB V-region; CDR3, complementarity determining region 3; TRBJ, TRB J-region.

*$p=10^{-7}$, Monte Carlo computations, MT TRB shared with tumor compared to WT TRB shared with tumor

Author Manuscript

Author Manuscript

Author Manuscript

**Table 4.**

Persistence of distinct TRB sequences[a] in blood and tumor of Patient 20.

| | T0 | | WT | | MT | |
|---|---|---|---|---|---|---|
| | **Blood** | **Blood & Tumor (% of total)** | **Blood** | **Blood & Tumor (% of total)** | **Blood** | **Blood & Tumor (% of total)** |
| 1 timepoint[b] | 27,576 | 189 | 13,095 | 119 | 617 | 55 |
| 2 timepoints[c] | 1,589 | 73 | 390 | 43 | 25 | 9 |
| 3 timepoints[c] | 387 | 43 | 87 | 18 | 10 | 5 |
| 4 timepoints[c] | 137 | 32 | 35 | 10 | 4 | 3 |
| 5 timepoints[c] | 118 | 44 | 32 | 16 | 0 | 0 |
| Total, persisting[d] | 2,231 | 192 (8.6%) | 544 | 87 (16.0%) | 39 | 17 (43.6%) * |
| Total, all timepoints[e] | 29,807 | 381 (1.3%) | 13,639 | 206 (1.5%) | 656 | 72 (11.0%) ** |

[a] distinct sequence as defined by nucleotide sequence and TRBV;

[b] # of sequences found in blood at only 1 timepoint;

[c] # of sequences found in blood at 2, 3, 4, or 5 sequential timepoints. Sequence were counted once under the highest category to avoid overcounting and overlap;

[d] Total # of sequences found in blood at any 2, 3, 4, or 5 sequential timepoints;

[e] Total # of sequences

TRB, T cell receptor beta; T0, time zero; WT; wild-type; MT mutant; IT-AG, intratumoral α-gal glycolipids.

* $p=10^{-4}$, Monte Carlo computations, MT TRB shared with tumor compared to WT or T0 TRB shared with tumor, persisting sequences.

** $p=10^{-7}$, Monte Carlo computations, MT TRB shared with tumor compared to WT or T0 TRB shared with tumor, sequences across all timepoints.